

# Draft

(submitted to the IAEATCM on Divertor Concepts  
Aix-en-Provence, Sept.11-14, 2001)

## Transport into and across the scrape-off layer in the ASDEX Upgrade divertor tokamak

**J. Neuhauser, D. Coster, H.U.Fahrbach, J.C. Fuchs, G. Haas, A. Herrmann, L. Horton, M. Jakobi, A. Kallenbach, M. Laux, J.W. Kim, B. Kurzan, H.W. Müller, H. Murmann, R. Neu, V. Rohde, W. Sandmann, E. Wolfrum  
and the ASDEX Upgrade Team**

Max-Planck-Institut für Plasmaphysik, EURATOM Association, Boltzmannstr. 2 D-85784 Garching, Germany

**Abstract.** The elements of transport into and across the scrape-off layer in the poloidal divertor tokamak ASDEX Upgrade are analyzed for different operational regimes with emphasis on enhanced confinement regimes with an edge barrier. Utilizing the existing set of edge diagnostics, especially the high resolution multi-pulse edge Thomson scattering system, in combination with long discharge plateaus, radial sweeps and advanced averaging techniques, detailed radial mid plane profiles of diverted plasmas are obtained. Profiles are smooth across the separatrix, indicating strong radial correlation, and there is no remarkable variation across the second separatrix either. Together with measured input, recycling, pumping and bypass fluxes, a corrected separatrix position is determined and transport characteristics are derived in the different radial zones generally identified in the profile structure. While transport in the steep gradient region inside and across the separatrix shows typical ballooning-type critical gradient scaling, though with deviations, the profile shoulders exhibit a more filamentary structure with preferential outward drift especially in high performance discharges, with formal diffusion coefficients far above the Bohm value in agreement with results on the old ASDEX experiment. A basic mechanism involved there seems to be partial loss of equilibrium and fast curvature driven outward acceleration, in principle well-known from theory, investigated decades ago in pinch experiments and utilized recently in high-field side pellet fuelling.

PACS numbers: 52.55.Fa, 52.40.Hf, 52.35.Ra

### 1. Introduction

The edge plasma layer in the vicinity of the magnetic separatrix of a poloidal divertor tokamak has a surprisingly strong influence on the global plasma performance especially in H-mode type discharges. The steep gradient and pedestal region forming just inside the separatrix controls the global energy confinement at least in case of stiff core temperature profiles [1]. Across the separatrix, this edge barrier region is intimately coupled to the diverted scrape-off layer (SOL), which directs the power flow mainly to the divertor target plates, while particles may flow predominantly to, and recycle from main chamber walls. A clear correlation is routinely observed in experiment between the core confinement and the recycling flux in the extreme edge [2]. Having identified the edge as a crucial player, it remains still unclear, which part is the most critical one, and what are the primary physical processes involved. The problem is further complicated by the fact that inside and across the separatrix most physically relevant radial scale lengths are of comparable size, e.g. the pressure decay length, gyro radius, banana width, radial mode correlation length, etc. coupling rather different modes and regimes, which we are normally used to discuss independently. A prerequisite to a careful analysis of the edge therefore is a detailed experimental input, which, in view of the edge complexity and limited experimental resources, is difficult to provide in reality.

In this paper we present and discuss edge measurement on the ASDEX Upgrade poloidal divertor tokamak with focus on main chamber radial profiles and basic radial transport mechanisms from the steep gradient

zone inside the separatrix out to the protection limiters. We first give an outline of the primary edge diagnostics and the plasma configurations primarily considered in this paper. Typical radial plasma profiles for different operational regimes are then presented and finally the elements of radial transport in different parts of the edge layer are qualitatively analyzed.

## 2. Edge diagnostics and plasma configuration

In ASDEX Upgrade [3] a number of diagnostics and analysis tools are available to investigate the edge region in great detail. The primary diagnostic used in this paper is the standard multi-pulse YAG laser Thomson scattering system [4], which can be positioned at the edge on purpose (figure 1). Six laser beams, each 2 mm wide, are launched vertically through the edge equally distributed in radial direction over a 15 mm wide interval. The lasers run at 20 Hz each, with an adjustable delay time between them. Normally, they are run equally spaced in time, (forming a 120 Hz pulse sequence). For the investigation of fast, transient phenomena, however, it is more appropriate to run them in burst mode with all six lasers close together (burst repetition rate of 20 Hz). The minimum time interval between subsequent lasers has been about 50 microseconds, but is being narrowed down to the microsecond level. The individual laser pulse length is only 20 nanoseconds, anyway. The scattered light is observed through a horizontal port in 16 vertically staggered channels. With the system positioned at the edge, channel 1 to 9 (counted from top downwards) measure in the edge layer in front of the antenna guard limiters, all others fall into the limiter shadow, with only the first few (up to 13) potentially useful in practice. An obvious advantage of (non-perturbing) laser light scattering is that electron temperature and density are obtained simultaneously at the same place without any mapping ambiguity. We shall come back to this point.

The radial electron density profile is measured in parallel with a fast Li-beam diagnostic [5]. The maximum sampling rate of the Li(2p) light is 25 kHz (with 5 mm radial channel width). Density profiles usually require averaging over typically 20 ms (with the option to cut out or overlay ELMs). The Li-beam is being used in parallel as charge exchange resonance spectroscopy (CXRS) source to obtain impurity ion temperature with 5 mm resolution, though only on a slow time scale. This allows a cross check and/or combination with the edge ion temperatures measured by the low energy neutral charge exchange analyzer (LENA [6]).

Neutral particle fluxes are measured at various toroidal and poloidal positions by encapsulated neutral pressure gauges with a small acceptance aperture [7]. Gas can be puffed in at various main chamber locations or through eight toroidally distributed divertor valves. There is a substantial bypass conductance ( $\approx 40 \text{ m}^3/\text{s}$ ) from the pumping plenum (housing a  $110 \text{ m}^3/\text{s}$  cryo pump and linked to external turbo molecular pumps with  $14 \text{ m}^3/\text{s}$ ) to the main chamber. Since the conductance between pumping and divertor chamber ( $\approx 70 \text{ m}^3/\text{s}$ ) is of similar size as the bypass, switching the cryo pump on and off allows to determine the corresponding global fluxes from the neutral pressure changes [8]. A fast reciprocating probe manipulator, accepting probe heads of different kind [9] is available in the mid plane, but is rarely operated because of limited manpower. In addition, there is a variety of diagnostics in the mid plane (e.g. spectroscopy) and divertor (e.g. thermography, Langmuir probes, spectroscopy. etc.) which are used occasionally in this paper, but cannot be described here in detail.

There is an approximately axisymmetric heat shield at the high field side, and 12 poloidal limiters at the low field side, essentially following the ion cyclotron antenna contour. All results reported are obtained in bottom single null configuration with the "closed" divertors Div II (LYRA) and Div IIb [8]. The conductances given above refer to Div IIb, but are similar for the LYRA. A specific plasma shape, with the low field side flux contour nearly fitting the antenna limiter contour is chosen for dedicated edge experiments, where possible. Figure 1 shows such a configuration together with a few diagnostics, especially the edge YAG system. Radial

plasma sweeps are routinely applied to extend the radial range, but also to check and eventually correct the relative laser channel calibration.

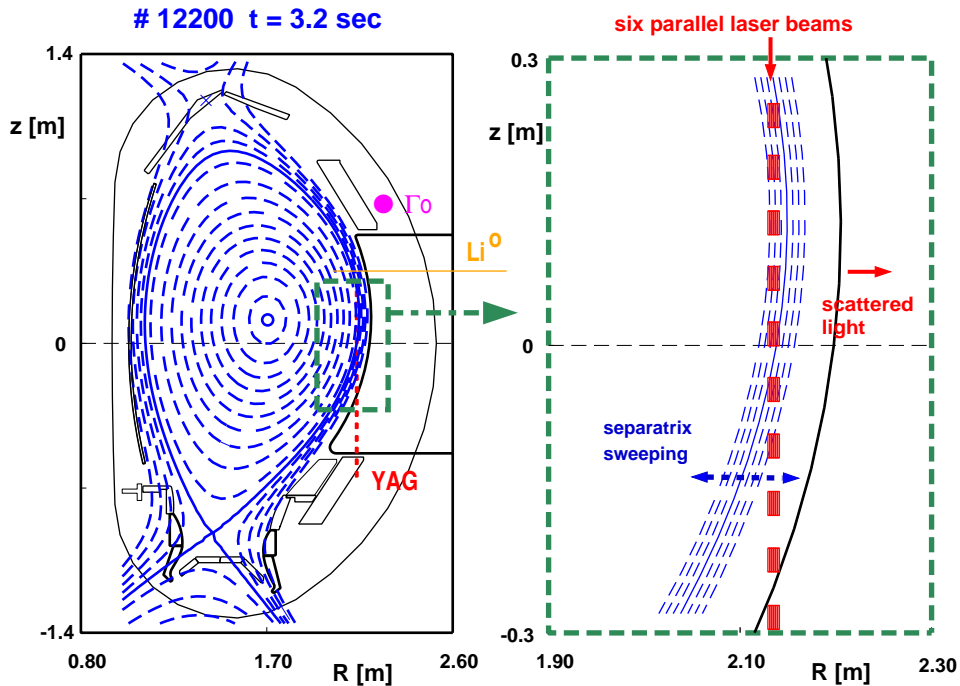


**Figure 1.** Poloidal cross section of ASDEX Upgrade (left part) together with equilibrium flux surfaces of the shot #12200 discussed extensively in this paper. The location of a few mid plane diagnostics is indicated ( $\Gamma_0$  = neutral flux measurement;  $\text{Li}^0$  = Li-beam; YAG = laser Thomson scattering channels, see also zoomed detail in the right part).

### 3. Radial plasma profile characteristics

A lot of information about radial transport can be obtained already from the radial profile structures together with the global power input and neutral recycling fluxes. Figure 2 shows electron density, temperature and pressure profiles in logarithmic scale from Thomson scattering for a medium triangularity H-mode discharge in deuterium with type-I ELMs (#12200,  $I_p = 1\text{MA}$ ,  $B_t = -2.5\text{T}$ ,  $q_{95} \approx 5$ ,  $P_{\text{NI}} = 5\text{MW}$ ,  $n_{\text{bar}} \approx 5.6 \cdot 10^{19}\text{m}^{-3}$ , about 67%  $n_{\text{GW}}$ , cryo pump off) extending from the pedestal inside the separatrix out to the guard limiters. The spatial coordinate  $x$  gives the distance from the nominal separatrix position along a horizontal line through the magnetic axis (positive values corresponding to the SOL). The separatrix position correction, as obtained from analytic heat conduction model fits to the temperature [10,11,12] or the B2.5 edge analysis code [13] or from B2-Eirene [14], is few millimeters only in most discharges, and practically negligible in #12200 (see below for more details). The distance to the outboard limiters is varied between 6 and 8 cm during the time interval chosen and there is a second separatrix about 2.5 cm outside the first one nearly independent of the sweep. All data points, including ELMs, are shown. The black dots represent box car averages (2 mm box width) calculated on the basis of Bayesian statistics [15]. The actual values depend somewhat on the assumptions for the experimental error, but the essential point is that this algorithm allows for a more reasonable treatment of outliers than simpler averaging techniques.

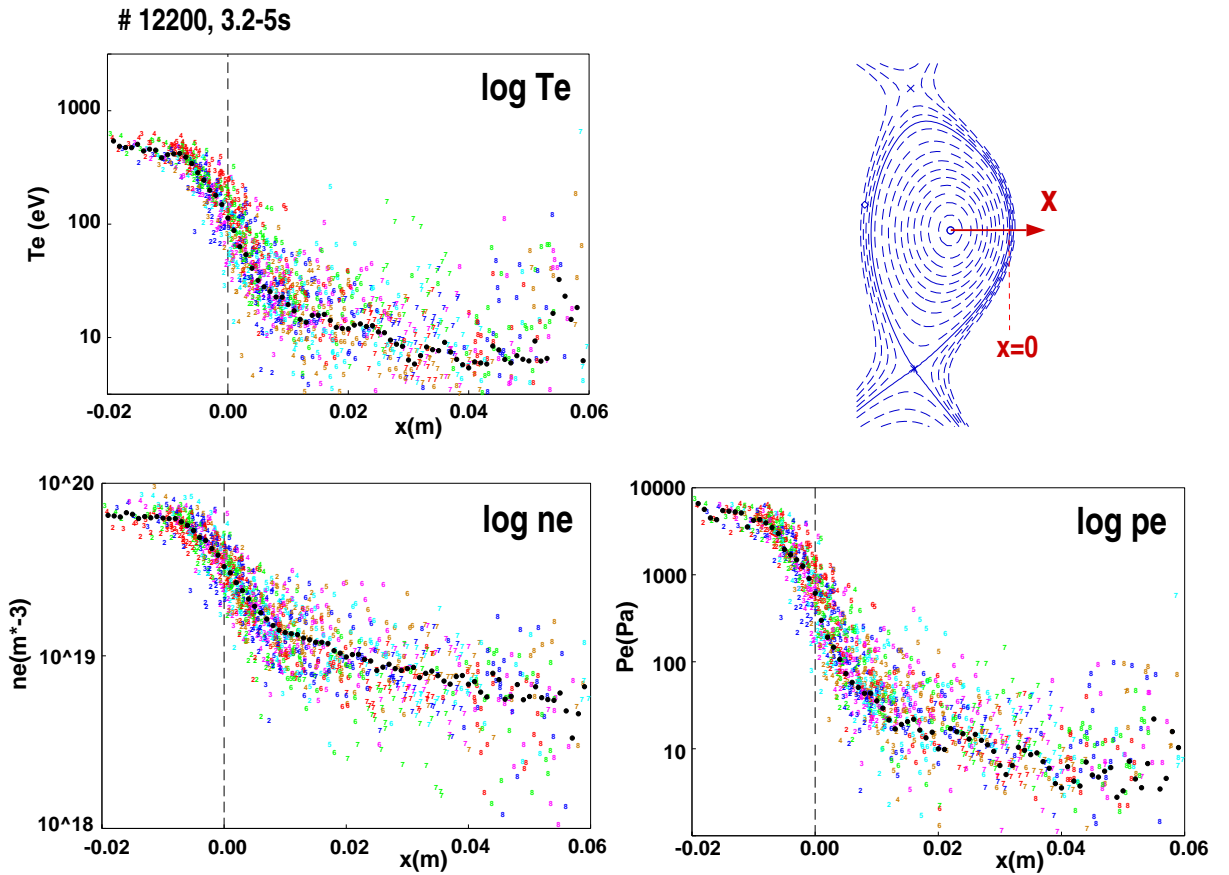


**Figure 2.** Mid plane profiles of electron temperature, density and pressure in logarithmic scale for the medium triangularity H-mode discharge # 12200 with type-I ELMs (see also figure 1). The definition of the coordinate  $x$  is indicated in the top right corner. All Thomson data obtained during a stationary discharge phase between 3.2 and 5 s. Numbers indicate different vertical channels and their colors identify the different lasers. The black dots represent Bayesian averages over a 2 mm radial interval.

Obviously, we can distinguish several qualitatively different radial regions which are likely to show rather different transport characteristics. The usual H-mode edge pedestal top [1], not further considered in this paper, is located near the inner end of the radial interval chosen. In outward direction it is followed by a steep gradient zone extending across the separatrix (about  $\pm 1$  cm), linking closed and open flux surfaces without any remarkable jump at the separatrix. Outside the hot scrape-off layer, the temperature is low and the average gradients become much flatter again, but now with increasing relative scatter. There is also no clear signature of the second separatrix on the profiles. A specific problem with SOL wing profiles is that the data scatter typically increases with decreasing average density, a behavior trivially expected in case of increasing instrumental noise, but also for high confinement discharges with steep gradient near the separatrix and a filamentary wing with transiently high local density. The smooth average wing density profile additionally shown in figure 2, the comparably low scatter in some low density L-mode edge profiles, statistical arguments and comparison with the Li-beam diagnostic (see below) indicate that noise may contribute, but is unlikely to be the dominant cause. An attempt with the new nanosecond laser light detection system to definitely separate physically relevant data, e.g. plasma vortices or filaments, from artifacts is under way [16].

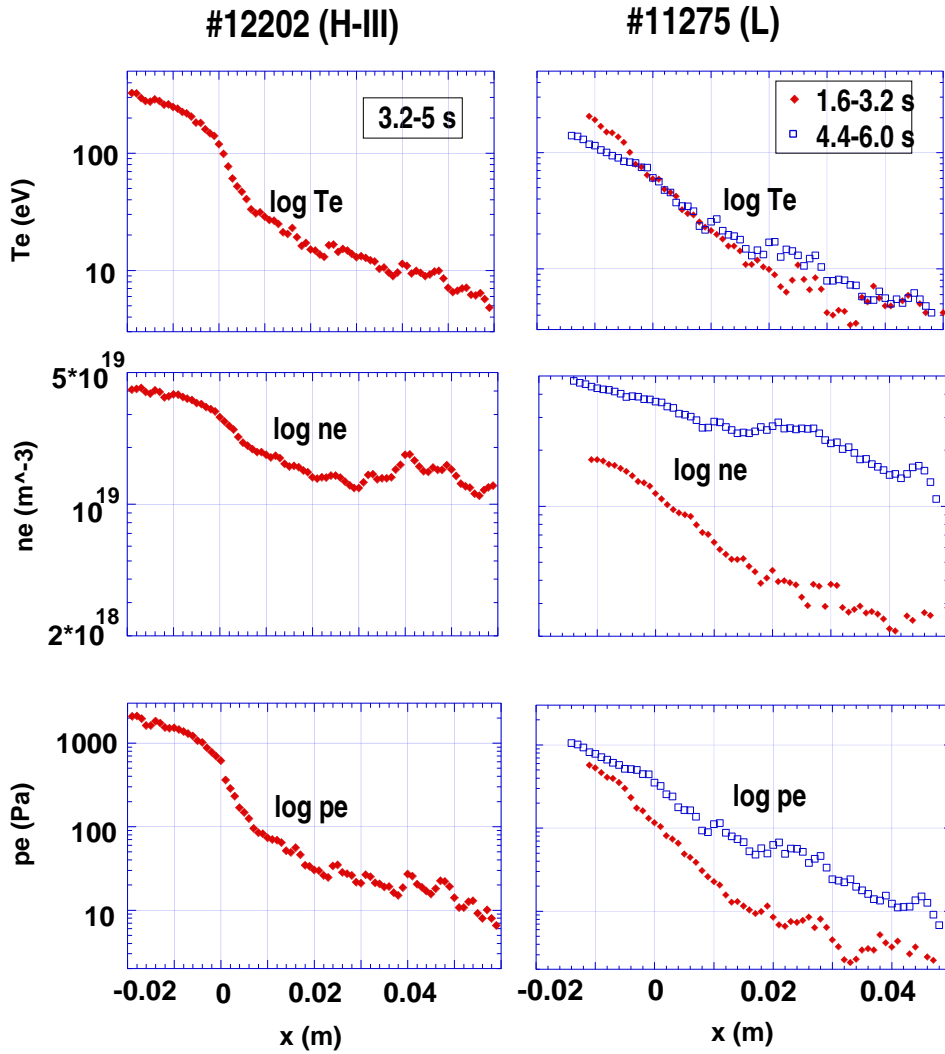


**Figure 3.** Mid plane profiles of electron temperature, density and pressure in logarithmic scale (Bayesian averages only) for the type-III ELMy H-mode deuterium discharge # 12202 (left) and the L-mode hydrogen discharge # 11275 (right). For the latter, two sets of profiles are given, corresponding to two subsequent density plateaus in the discharge.

The described profile structure is qualitatively recovered in practically all H-mode-type discharges analyzed, but there are, of course, clear quantitative variations with major operational parameters, like density, plasma current etc. As another H-mode example, we show in figure 3 (left) the average profiles of the type-III ELMy discharge #12202 ( $I_p = 0.6\text{MA}$ ,  $B_t = -2.5\text{T}$ ,  $q_{95} \approx 8$ ,  $P_{\text{NI}} = 5\text{MW}$ ,  $n_{\text{bar}} \approx 8.5 \cdot 10^{19}\text{m}^{-3}$ , about 75%  $n_{\text{GW}}$ , cryo pump off). Because of lower current, the discharge is closer to the density limit although the core density has been lowered, too. Nevertheless, the absolute scrape-off layer wing density is even increased relative to #12200 (with virtually zero density gradient over a few cm similar to earlier observations [17, 18]), making the profile altogether flatter, but there is still a steep region across the separatrix.

Apart from the absence of a pronounced pedestal, this radial structure also appears in L-mode discharges as shown in figure 3 (right) for a low-triangularity hydrogen discharge #11275 ( $I_p = 1\text{MA}$ ,  $B_t = -2.5\text{T}$ ,  $q_{95} \approx 4.3$ ,  $P_{\text{NI}} = 3.5\text{MW}$ ,  $n_{\text{bar}} \approx 4.1 \cdot 10^{19}\text{m}^{-3}$  and  $7.3 \cdot 10^{19}\text{m}^{-3}$ , about 33% and 62%  $n_{\text{GW}}$ , resp., cryo pump off). The profiles are taken during a radial position scan with the closest local separatrix-limiter distance

varying between 3.5 and 5 cm, but a larger gap of 5 to 7 cm at the Thomson diagnostic location (again only the Bayesian averages are shown).

Edge ion temperatures obtained from low energy charge exchange neutrals (LENA diagnostic plus Eirene neutral particle Monte Carlo code [6]) are usually close to the electron temperature for the medium and high density H-mode discharges predominantly run at ASDEX Upgrade. The ion temperature (and pressure) gradients, however, have substantial error bars as a result of the complex unfolding procedure, but also because of possible deviations of the local ion distribution function from a Maxwellian assumed in the unfolding algorithm. First results from the new high-resolution Li-beam CXRS have confirmed the absolute LENA temperature level, but, by accident, did not cover the steep gradient zone indicated by the LENA analysis. Therefore we leave the detailed edge ion transport discussion to a future paper.

#### 4. Transport across the separatrix and separatrix position

From simple physical arguments, we might expect a strong change of transport in the edge when moving from closed magnetic flux surfaces across the separatrix to ‘open’ ones, intersecting material walls and defining the scrape-off layer. For such a jump in the transport coefficient, simple diffusive radial transport models would predict a jump in the *first* derivative across the separatrix (because of flux continuity), while for a continuous transport only the *second* derivative jumps because of the onset of parallel loss. From the experimental mid plane profiles there is no indication for a jump in gradients at the nominal separatrix position (determined by equilibrium reconstruction from magnetic measurements). Our first non-trivial conclusion is therefore that transport across the separatrix is about continuous. The most likely physics behind is a finite radial transport correlation length of the order of a centimeter in agreement with experimental results [19, 20] and 3-dimensional turbulence simulations [21], smoothing profiles across the boundary even if the dominant instability drive is asymmetric relative to the separatrix. The latter still needs to be discussed in more detail.

This continuity means also that the separatrix cannot trivially be identified from radial profiles, and we must check and determine the separatrix self-consistently, in order to draw the right physical conclusions. (The most rapid variation near the separatrix in low power discharges is usually seen in the floating potential from Langmuir probes [9], but probes cannot be applied in these hot edge plasmas and there are also unexplored perturbing effects on the electric field e.g. from magnetic field ergodisation and from the probe itself). Once we have adopted a transport model, we can check and correct the separatrix position as part of the model validation process. This has been done on different levels, with the electron temperature at the separatrix as a key parameter. A fit of the electron temperature profile with analytic solutions of a simple 1.5 d edge heat conduction model with different cross field transport has been routinely applied yielding corrections (mapped to the mid plane) in the few mm range, occasionally up to about 2 cm, consistent with further diagnostic checks (e.g. separatrix hit points on divertor targets from thermography) [10, 11]. Applying advanced statistical methods, it even seems possible to sort out the most likely transport law, e.g. a more Bohm-like scaling for high density, but a more constant heat transport coefficient  $\eta_{\chi}$  for low density discharges [12].

Much more complete physics models are used in numerical edge transport codes, e.g. the edge analysis code B2.5-I [13], fitting all mid plane profiles and a selection of divertor data, neutral fluxes, etc. Nevertheless, the corrected separatrix agrees with the equilibrium reconstruction within an obviously unavoidable residual error band of a few mm width. Higher accuracy seems to be irrelevant anyhow in view of finite physical scale lengths like ion toroidal and poloidal gyro radius, deviation of drift surfaces from magnetic surfaces of the same order, or ergodisation of field lines by external error fields over a few mm (all distances refer to low field side mid plane). Ergodisation is also caused by internal edge turbulence, but 3-dimensional turbulence

codes reveal that radial transport is still dominated by cross field motion rather than along ergodic field lines even for electron energy [21].

The advantage of the non-perturbing Thomson scattering for separatrix determination and model validation is that electron density and especially temperature (and hence pressure) are determined exactly at the same location and time. In contrast, it is practically impossible to get the local separatrix from the Li-beam diagnostic itself, measuring density (and eventually ion temperature) profiles at a different toroidal position. The solution adopted therefore is cross calibration of steep density profiles from laser and Li-beam, which in fact revealed a misalignment (or equilibrium distortion) of about one centimeter [22]. A comparison of the density profiles for #12200 from Thomson scattering and the (1 cm shifted) Li-beam diagnostic in between ELMs (i.e. cutting out ELMs in both diagnostics) is shown in figure 4. A shorter discharge time interval has been selected during which the nearest distance to the outside limiters varies between 7.5 and 8 cm only.

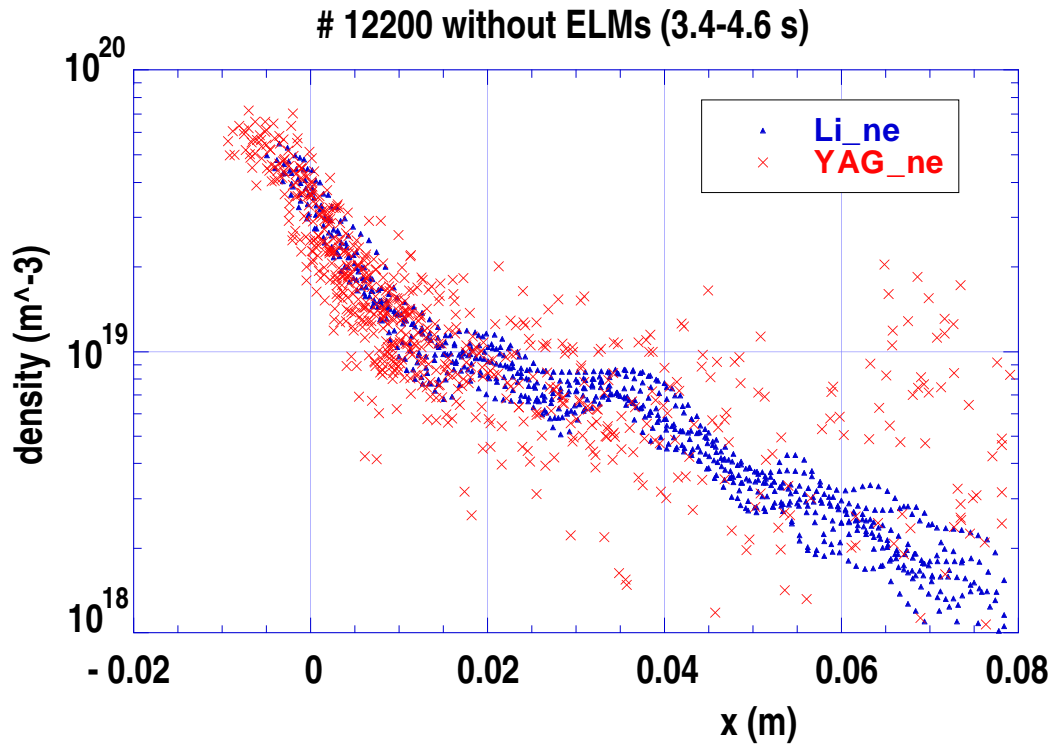


**Figure 4.** Comparison of density profiles from Thomson scattering and the Li-beam diagnostic for discharge #12200. ELMs are cut out in both diagnostics. For the Li-beam several profiles during the same time interval are overlaid, each with a 20 ms time average (leaving out the ELMs). During the selected time interval the plasma sweep is only about 5 mm. In the figure, the corresponding limiter position relative to the separatrix is therefore at 7.5 to 8 cm.

An edge data base including electron temperature from Thomson scattering, ELM averaged densities from the (not yet position corrected) Li-beam combined with core DCN interferometer, and various other parameters (neutral fluxes, divertor data, heating and radiation loss, etc.), had been established some time ago. This data were analyzed with B2.5-I and preliminary scalings of various quantities, especially of cross field transport coefficients have been presented [13]. The profile fit was restricted to about  $\pm 1$  cm around the separatrix by a weighting function on the residuals to be minimized, and only one fitting parameter per transport channel (and free separatrix position as discussed) was chosen. The rationale behind was the radial transport correlation mentioned above and the success of previous analytic model fitting over the same

interval. For instance, regression of the heat transport coefficient with respect to engineering parameters revealed a strong magnetic field dependence and a nearly linear SOL power dependence, similar to what would be expected from a critical gradient limitation by pressure driven modes, e.g. ideal or resistive ballooning modes as discussed in the pedestal literature [23].

Obviously, the same mechanism prevails in the separatrix vicinity, though formally the global magnetic shear, a key element in simple ballooning theory, diverges. In a real divertor configuration like figure 1, however, the local shear is rather small in the bad curvature region (depending e.g. on the amount of local bootstrap current), being concentrated near the x-points instead. Assuming for simplicity a double null configuration with both x-points on the same flux surface with a connection length  $L_c$  between them, we can construct a criterion for marginal stability near the separatrix by comparing the destabilizing force originating from the pressure gradient with the restoring force from finite wavelength field line bending. In a simple plasma loaded string model, the marginal point is obtained by equating the ideal ballooning growth rate  $\gamma^2 \approx v_i^2 / (R \lambda_p)$  with the stable kink mode frequency  $\gamma^2 \approx (k v_a)^2$ ,  $k \approx \pi / L_c$  ( $v_i$  = ion thermal velocity,  $v_a$  = Alfvén velocity,  $\lambda_p$  = pressure decay length). The result can be rewritten as a critical total pressure gradient  $p_{crit} / \lambda_p \approx p^2 R B^2 / (\mu_0 L_c^2)$  similar to the ballooning limit obtained for circular cross section and numerically of the order of the experimental one.

This estimate seems to explain qualitatively also the marked increase of the pressure gradient near the separatrix from low triangularity single null towards high triangularity double null as routinely observed in ASDEX Upgrade [23]. While the simple ballooning estimate yields for a given equilibrium configuration the usual  $B^2$  scaling of the critical edge gradient just inside the corrected separatrix, we find experimentally in such a B-scan at constant-q a lower dependence, approximately  $B^{1.5}$ . Though the reason might be a slight change in flux surface geometry and edge shear, since the total stored energy scales linearly only with  $B$ , it is more likely that this deviation just indicates a more complicated physics with different mechanisms mixed in this narrow steep gradient layer as mentioned in the introduction.

Magnetic shear becomes ineffective, if the electric resistance exceeds a critical value allowing for sufficiently rapid field line reconnection in the sheared region. This may partly explain the decrease of the separatrix pressure gradient with increasing collisionality, resulting finally in a H-L back transition approximately coinciding with strongly increased x-point radiation cooling. Since such a critical collisionality appears in many edge related mechanisms like resistive mode turbulence, line tying at target plates and divertor detachment, a final assessment of the dominant effect seems premature, despite encouraging progress in edge turbulence codes with realistic separatrix geometry [24].

## 5. Transport and recycling in the cold scrape-off layer part

Moving away from the hot SOL into the cold (e.g.  $T_e \leq 20$  eV) SOL wing, there is a clear profile flattening indicating a significant increase of radial transport. This effect has been observed already in the old ASDEX experiment [25, 17, 20] and was immediately recovered in the early days of ASDEX Upgrade [18]. 2-dimensional numerical edge modeling with B2 and B2-Eirene, resp., revealed a rapid anomalous transport in this region towards the wall, factors above and hence in contradiction to Bohm diffusion, which is usually thought to be an upper limit of electrostatic turbulence. Alternatively, a rapid outward pinch velocity (70 m/s) was formally used [18], based on the idea that the violation of the Bohm diffusion limit should indicate a preferential outward  $\mathbf{E} \times \mathbf{B}$  drift of filamentary structures rather than small scale diffusion. The nearly instantaneous Thomson data in comparison with the time-averaged densities from the Li-beam light emission seem to support this idea quite in detail.

We start our analysis with a formal estimate of radial particle transport coefficients from a simple, qualitative model: The measured main chamber neutral recycling flux  $\Gamma_0$  hits the plasma, is converted to atoms via Franck-Condon processes with a penetration depth in terms of integral density of  $2 \cdot 10^{18} \text{ m}^{-2}$  (and partly

reflected by charge exchange, e.g. albedo  $\approx 0.5$ ). Assuming an equal, but opposite flow of ions and knowing the local charged particle density we trivially get an effective outward transport velocity  $v_{\text{out}}$  under the preliminary assumption that there is negligible loss to the divertor. With  $\Gamma_0 \approx 10^{21}$ ,  $2.4 \cdot 10^{21}$ ,  $2.4 \cdot 10^{20}$  and  $1.85 \cdot 10^{21} \text{ m}^{-2} \text{ s}^{-1}$  for #12200, #12202, and #11275 (low and high density part), we find roughly  $v_{\text{out}} \approx 50$ , 80, 24 and 45 m/s, respectively, at a position a few centimeter away from the separatrix. These values increase further towards the wall, but decrease rapidly towards the core, since the flux decreases inward by absorption, while the density rises.

Multiplying  $v_{\text{out}}$  by the local density decay length yields formal wing diffusion coefficients between about  $1 \text{ m}^2/\text{s}$  and virtually infinity, well above Bohm diffusion (about  $0.3 \text{ m}^2/\text{s}$  at 10 eV) in agreement with former experience. The lowest discrepancy holds for the low density L-mode phase of #11275 (fig. 3, right), while the extreme values refer to the essentially horizontal shoulders of the type-III ELMy H-mode discharge #12202 (fig. 3, left) and the high density L-mode (fig. 3, right). Obviously the concept of a local diffusive transport driven by small scale turbulence in a smooth quasi-static background equilibrium plasma is no longer valid for this highly turbulent, filamentary region.

With the radial transport velocities given above, the average transport time through the cold SOL wing is about a millisecond. The competing flow time to the top and bottom divertors or divertor throat structures (see figure 1) along field lines at sonic speed would be similar. However, the field line integrated neutral density is of order  $10^{20} \text{ m}^{-2}$ , i.e. an ion with thermal speed would undergo many ( $\approx 50$ ) charge exchange collisions along this way, losing its momentum on a short distance. In other words, neutral friction will result in much slower, subsonic flow (Mach number  $M \ll 1$ ), and the assumption of predominantly radial recycling flow is justified in agreement with numerical simulations [13, 14].

$M \ll 1$  prevails also in the hot SOL near the separatrix, even in the absence of main chamber neutrals, because of localized high recycling in the closed bottom divertor. Nevertheless, the global flux balance indicates that, because of the bypass conductance together with the high divertor neutral pressure, the total residual flux into the divertor may still be a substantial fraction (e.g. 20%) of the total main chamber recycling flux, even with the cryo pump off [8]. The average cross field convective energy transport to the limiters including charge exchange is proportional to  $\Gamma_0$  and typically of the order of  $10 \text{ kW}/\text{m}^2$  or a few hundred kW total, far below the heating power.

In figure 4, we had compared Li and YAG density profiles. While we could obtain quite reasonable agreement near the separatrix by an appropriate radial shift, the Thomson scattering gives remarkably higher values in the outer profile wing. This difference may tell us an interesting piece of physics, since the two diagnostics result in different density averages in case of large amplitude density variations. In contrast to the Li-beam diagnostic, which yields the normal time average, the laser pulses produce data points only, if the scattered light is above a certain level needed to derive valid temperature and density values. Therefore, for e.g. near 100% density fluctuations or single plasma blobs, the Thomson values are more typical for the maximum event density rather than the simple time average as obtained from the Li-beam. The true peak density is even higher for plasma filaments, which do not fill the whole scattering volume (2 mm radial by 25 mm vertical), e.g. by a factor of five for a centrally hit filament with 5 mm diameter. In addition, the fraction of valid data points (about 50% in the scattered data region, nearly 100% elsewhere) gives an indication for the event statistics. As seen in figure 2, typical mean data of such plasma fluctuations or local filaments in #12200 are a density of about  $10^{19} \text{ m}^{-3}$  and a temperature around 10 eV, corresponding to a charged particle mean free path of  $\lambda_{\text{mfp}} \approx 0.2 \text{ m}$ , with large relative scatter around these values.

In principle, such low energy SOL plasmas are easy to investigate by Langmuir probes. In fact, a comprehensive study of SOL fluctuations and filament-type events has been done on the old ASDEX experiment and a simple model including the electrostatic sheath at the target plates has been presented [20]. These measurements and their interpretation are consistent with the ASDEX Upgrade finding reported here.

Since such a similarity had been anticipated and because of lack of man power, these SOL turbulence measurements were not repeated in detail at ASDEX Upgrade up to now.

A minority of surprisingly high temperature values (not correlated with ELMs) are found in the outer SOL, comparable to those near or even inside the separatrix. If these structures would, in fact, originate from this hot region and drift across open field lines, they would have to move fast enough to avoid electron cooling along field lines. Assuming flux limited heat transport to the target plates in a plasma filled flux tube with a length of 30 m and a temperature of 100 eV, we get a cooling time of the order of 30 microseconds. In order to survive a 3 cm displacement, an average radial ExB velocity beyond 1000 m/s is needed, equivalent to a poloidal electric field of a few kV/m, qualitatively consistent with a potential drop of the order of  $kT/e$  over a filament diameter. These numbers are again similar to those found in [20] for old ASDEX.

Since there is essentially the same physics behind, it is not surprising that these numbers are also consistent with the theoretical acceleration of a diamagnetic plasmoid in a curved magnetic field,  $b \approx 4kT/mR$  ( $\approx 10^{10} \text{ ms}^{-2}$  for 100 eV), a basic mechanism experimentally confirmed decades ago in toroidal theta pinches and exploited in high field side pellet injection [26, and refs therein]. For sufficiently high temperature, the magnetic flux may be partly frozen to the plasma causing field line bending and hence a restoring force as considered above in the simple kink model. As outlined in [26], the maximum deflection in the infinite conductivity limit is proportional to the filament beta. Since the true filament pressures in the SOL wing may be a factor of 5 higher than the values given in figure 2 as mentioned, displacements in the centimeter range are not impossible even in this limit. However, in contrast to filamentary plasmoids created by pellet injection, it is less clear, how macroscopically drifting filaments are generated in a turbulent steep gradient edge plasma. A quantitative assessment of the physical mechanisms will require fully nonlinear, electromagnetic turbulence simulation with a model including all the physical and geometrical effects indicated above. Finally, for curiosity, but also in support of our present interpretation, we would like to refer to old theta pinch work at Garching, where filament formation, separation from the plasma column and decay, forming finally a cold ( $\approx 5 \text{ eV}$ ) halo around the core plasma, has been routinely observed on a microsecond time scale during compression oscillations e.g. by fast streak cameras [27].

Far edge transport and main chamber recycling has gained renewed interest recently in the USA. A rather detailed edge transport analysis for C-mod has been given by LaBombard [28]. Qualitative estimates for the dynamics of isolated filaments and the associated transport have been presented in [29]. Though there are differences in various details, the major experimental findings and their interpretation seem to be consistent with the ASDEX / ASDEX Upgrade picture.

## 6. Conclusions

Based, to a large extent, on high resolution profiles from the edge Thomson scattering system, we have qualitatively analyzed and discussed the elements of transport into and across the scrape-off layer in ASDEX Upgrade poloidal divertor discharges. In support, other diagnostics and reference to previous ASDEX and ASDEX Upgrade related work on specific aspects have been given, wherever appropriate.

Robust profile and transport characteristics like steep gradients inside the separatrix and strongly enhanced transport in the outer SOL wing, known already from previous work, were confirmed. Beyond that, the remarkable accuracy obtained now e.g. by averaging over long discharge plateaus and introducing radial position scans, in combination with the short pulse length of the six lasers, staggered in space and time, reveal much more details. Models and tools of different levels of sophistication are used e.g. to determine the most likely separatrix position and to treat strongly scattered data.

A clear transport correlation has been found from the steep gradient layer across the separatrix into the hot part of the SOL. Pressure gradients and transport scalings are approximately ballooning-like, but deviate in

detail from those predicted by simple models as discussed in the H-mode literature. This is not unexpected in view of the edge complexity and especially the extreme parameter variation over a short radial distance, probably causing a strong mixing and coupling of modes, which are usually treated separately in theory. However, more robust features like the basic field aligned mode structure, the localization of shear stabilization near the x-points and its dependence on collisionality are supposed to prevail and still to determine the scaling qualitatively.

Outside the hot SOL, there is a rapidly increasing effective transport far beyond the Bohm diffusion usually taken as the upper limit of electrostatic cross field transport. The filamentary structure, the large average outward velocity even for flat profiles, and the possibly extreme speed of a minority of hot filaments indicate that a local diffusive transport model is inappropriate in this region. This rapid SOL wing transport causes practically a short circuit between the hot, low transport barrier in the separatrix vicinity and the outboard limiters. This interpretation may at least partly explain the surprisingly clear correlation of various quantities in the far SOL wing with core confinement and global plasma performance in H-mode: Towards inside, the steep gradient and pedestal layer controls the core plasma via profile stiffness. The same layer determines the fueling (and wall recycling) flux needed from outside to establish a desired core plasma density. Because of the effective short circuit to the wall, the actual wall distance is then unimportant as long as the hot layer is unaffected. This is confirmed by the radial position sweeps leaving, for instance, the ELM signature and the stored energy completely unchanged, if the gap to the wall is larger than the width of the hot, steep gradient SOL region.

## References

- [1] W. Suttrop et al.; Plasma Phys. Control. Fusion 39 (1997) 2051
- [2] A. Kallenbach et al.; Plasma Phys. Control. Fusion 41 (1999) B177
- [3] Gruber, O., et al.: in Fusion Energy 1998 (Proc. 17<sup>th</sup> Int. Conf, Yokohama 1988), Vol.1, p.213, IAEA, Vienna, 1999.
- [4] B. Kurzan, H. Murmann, H. Salzmann, and the ASDEX Upgrade Team, Rev. Sci. Instrum. 72 (2001) 1111.
- [5] S. Fiedler et al.; J. Nucl. Mater. 266-269 (1999) 1279
- [6] Stober, J., et al.: Plasma Phys. Control. Fusion 39 (1997) 1145.
- [7] G. Haas, H.-S. Bosch, Vacuum 51 (1998) 39
- [8] R Neu et al.; "Properties of the new divertor IIb in ASDEX Upgrade", this conf
- [9] V. Rohde et. al.; Contrib. Plasma Physics, 36 (1996) S 109 (special issue).  
V. Rohde et al.; J Nucl. Mater. 241-243 (1997) 712
- [10] J. Schweinzer et al.; J. Nucl. Mater. 266-269 (1999) 934
- [11] Neuhauser, J., et al.: ECA Vol. 23J (1999) 1521 (26<sup>th</sup> EPS Conf. on Controlled Fusion and Plasma Physics, Maastricht, Netherlands).
- [12] V. Dose et al.; "Tokamak edge profile analysis employing Bayesian statistics", Nuclear Fusion (2001), accepted for publication
- [13] J.W. Kim, D.P. Coster, J. Neuhauser, R. Schneider, ASDEX Upgrade Team, J. Nucl. Mater., 290-293, (2001) 644-647.
- [14] Coster, D. P., et al.: Contrib. Plasma Phys. 40 (2000) 334.
- [15] V. Dose and W. von der Linden, "Outlier Tolerant Parameter Estimation",  
W. von der Linden et al. (eds.), Maximum Entropy and Bayesian Methods, 47-56, Kluwer Academic Publishers (1999).

- [16] M. Jakobi et al.; "Measurements of fast local changes in electron temperature and density by Thomson scattering at ASDEX Upgrade"; abstract submitted to APS conference 2001
- [17] J. Neuhauser et al., Plasma Phys. Contr. Fusion 31 (1989) 1551
- [18] H.-S. Bosch et al., J. Nuclear Mater 220-222 (1995) 558
- [19] B. Kurzan et al.; Plasma Phys. Control. Fusion 42 (2000) 237
- [20] M. Endler et al., Nuclear Fusion 35 (1995) 1307
- [21] B. Scott, Plasma Phys. Control. Fusion 39 (1997) 471
- [22] H.W. Müller et al.; 28<sup>th</sup> EPS conference on Controlled Fusion and Plasma Physics, Madeira (2000); contributed paper P1.109
- [23] W. Suttrop et al.; Plasma Phys. Control. Fusion 42 (2000) A 97
- [24] X.Q. Xu et al.; Nuclear Fusion 40 (2000) 731
- [25] K. McCormick et al.; J. Nucl. Mater. 145-147 (1987) 215
- [26] H. W. Müller et al.; Phys.Rev.Lett. 83 (1999) 2199
- [27] J. Freund, Report IPP1/125 (1972), Max-Planck-Institut für Plasmaphysik, Garching
- [28] B. LaBombard, et al., Nuclear Fusion 40 (2000) 2041
- [29] S.I. Krashenninkov; Physics Letters A 283 (2001) 368